105, 4481 (1983); C. D. Bain and G. M. Whitesides, *Angew. Chem. Int. Ed. Engl.* **28**, 506 (1989), and references therein; G. M. Whitesides and P. E. Laibinis, *Langmuir* **6**, 87 (1990), and references therein.
3. We use the term "feature" to mean a region of the surface with a property that is distinguishable from its surroundings.
4. The Au substrates were prepared by evaporation of 100 Å of Ti (99.999%) onto a polished Si(100) wafer (Silicon Sense, Nashua, NH) followed by 2000 Å of Au (99.999%) with an electron beam evaporator operating at a pressure of approximately 10^{-6} torr.
5. C. D. Bain and G. M. Whitesides, *Langmuir* **5**, 1370 (1989); S. R. Holmes-Farley, C. D. Bain, G. M. Whitesides, *ibid.* **4**, 921 (1988).
6. The depth and width of the micromachined grooves could be controlled by varying the load (1.2 to 9.8 mN) on the tip of the scalpel blade (Feather Industries, Tokyo) and carbon fiber (diameter, 8 μm). By using energy-dispersive x-ray fluorescence measurements, we detected no evidence of exposed Si within the micromachined groove.
7. The plastic deformation of the Au suggests that the machining pressure exceeded the yield strength of the Au. If we assume a scalpel tip area of 10 μm^2 in contact with the Au surface, a load of 3 mN corresponds to a tip pressure of 300 MPa. This pressure is greater than the yield strength of bulk Au (3.4 to 14 MPa, depending on thermal history) and comparable to the ultimate tensile strength of bulk Au (131 MPa) [E. M. Wise, *Gold: Recovery, Properties, and Application* (Van Nostrand, New York, 1964)].
8. Scanning electron microscopy (SEM) images of the tip of the carbon fiber showed a morphology resembling thin parallel sheets. These tips sometimes formed distinct parallel grooves, separated by as little as 0.1 μm.
9. By using a dialkyl disulfide to form the second SAM, the exchange with thiolates of the first SAM can be reduced to less than 0.1%. For example, a SAM formed from $CH_3(CH_2)_{10}SH$ has been measured, by using the contact angles of water on the SAM and x-ray photoelectron spectroscopy, to exchange less than 0.1% when exposed to a 0.1 mM solution of $[HO(CH_2)_{11}S]_2$ in ethanol for 10 s at 25°C (H. A. Biebuyck and G. M. Whitesides, unpublished results).
10. We have also formed the second SAM using a 0.1 mM solution of $CF_3(CF_2)_9(CH_2)_2SH$ in ethanol and very short (~1 s) adsorption times. The rate of reaction of $CF_3(CF_2)_9(CH_2)_2SH$ with the bare Au is faster by a factor of 10 than the rate of its exchange into the first SAM [C. D. Bain *et al.*, *J. Am. Chem. Soc.* **111**, 321 (1989); C. E. D. Chidsey, C. R. Bertozzi, T. M. Putvinski, A. M. Mujsce, *ibid.* **112**, 4301 (1990); D. M. Collard and M. A. Fox, *Langmuir* **7**, 1192 (1991); C. D. Bain, H. A. Biebuyck, G. M. Whitesides, *ibid.* **5**, 723 (1989)].
11. Although grooves formed with a load of 3 mN applied to the tip of the scalpel did not pin the edges of drops, grooves formed with larger loads (≥10 mN) showed a weak tendency to pin drops. Because larger loads produce larger grooves, this suggests that the shapes of the grooves can influence the pinning of drops.
12. Top views of the drops under an optical microscope indicated that the separation of the drops was ≤5 μm.
13. These observations are consistent with the established influence of "surface roughness" (including grooves) on the wetting of solid surfaces with liquids [P. G. de Gennes, *Rev. Mod. Phys.* **57**, 827 (1985), and references therein].
14. Drops of water can also be pinned by "writing" lines of SAMs with liquid alkanethiols. In this case there is no deformation of the surface (H. A. Biebuyck and G. M. Whitesides, unpublished results).
15. We use the term "optical lithography" to mean lithography with radiation wavelengths in the range 248 nm (KrF excimer laser) to 436 nm (mercury arc source) [J. Bruning, *Opt. Photonics News* **2**, 23 (May 1991)].
16. The rate of lateral diffusion of molecules in the SAM is unknown but may ultimately limit the resolution of the method.
17. P. E. Laibinis, J. J. Hickman, M. S. Wrighton, G. M. Whitesides, *Science* **245**, 845 (1989).
18. The analysis of wetting in the corners can yield fundamental information such as the contact angle of the liquids on the SAMs.
19. Supported by the Office of Naval Research and the Defense Advanced Research Projects Agency. SEM images were obtained at the Harvard University Materials Research Laboratory. We thank H. A. Biebuyck for helpful suggestions and insightful discussions.

17 April 1992; accepted 8 July 1992

The *Autographa californica* Baculovirus Genome: Evidence for Multiple Replication Origins

Margot Pearson, Rebecca Bjornson, George Pearson, George Rohrmann*

The *Autographa californica* multinucleocapsid nuclear polyhedrosis virus (AcMNPV), which is used for the overexpression of eukaryotic genes and is being engineered for possible use as a viral insecticide, has a circular, supercoiled genome of approximately 128 kilobases. Despite its widespread use, little is known about the mechanism by which AcMNPV replicates. Evidence is presented in this report that AcMNPV origins of DNA replication are repeated sequences each containing several closely related imperfect palindromes that are present in six regions distributed around the genome. Although AcMNPV infection–dependent plasmid replication was initiated by a single complete palindrome, the amount of replication was substantially increased in plasmids containing six or eight palindromes.

The AcMNPV genome contains a series of six homologous regions (*hrs*) designated *hr*1 through *hr*5 (*hr*4 contains two *hrs*, designated *hr*4L and *hr*4R, that are separated by 4 kb of DNA) (*1*–*3*). The five major *hr* regions vary in size from 0.4 to 1.0 kb and are separated on the AcMNPV genome by about 25, 42, 19, 15, and 15 kb of DNA, respectively (Fig. 1A). Each *hr* region contains from two to eight (for a total of 33) 30-bp imperfect palindromes with naturally occurring Eco RI sites at their core (Fig. 1B) (*3*). The palindrome sequences exhibit the following properties: (i) They have an invariant 10- to 12-bp core sequence. (ii) There are two areas of mismatches at 4 or 5 bp and 10 or 11 bp from each Eco RI site. (iii) They are separated by about 83 ± 34 bp. (iv) They act as transcriptional enhancers (*2*, *3*). Cochran and Faulkner (*1*) originally suggested that *hrs* may be baculovirus replication origins. To test this hypothesis, we transfected a plasmid containing the Hind III-Q fragment into AcMNPV-infected *Spodoptera frugiperda* (Sf9) cells. This fragment contains *hr*5, which consists of six palindromes distributed over about 600 bp of DNA (Fig. 1, A and B). DNA was subsequently extracted from the infected cells and subjected to digestion by the endonuclease Dpn I, which exclusively cleaves the fully methylated restriction site (GmeATC) (*4*). The Dpn I sites of bacterially produced plasmid DNA are fully methylated and can be cleaved by Dpn I. The sites in DNA replicated in eukaryotic cells are not methylated and are not digested by Dpn I. Therefore, Dpn I is used to differentiate between input plasmid and plasmid DNA that has replicated in the eukaryotic cells (*5*). In this initial experiment, we found the plasmid containing *hr*5 was amplified and became Dpn I–resistant after transfection into AcMNPV-infected Sf9 cells indicating that it had replicated. The vector, pBluescript (pBKS$^-$, Stratagene, La Jolla, California), was not replicated under these conditions.

We constructed a series of deletion mutants from the AcMNPV Hind III-Q region that yielded plasmids containing six, four, two, one, and an incomplete palindrome (Fig. 1, A and B). Individual constructs were transfected into AcMNPV-infected Sf9 cells. After 65 hours, total cellular DNA was extracted and was digested with Dpn I and then by Eco RI to linearize remaining plasmid DNA to facilitate analysis. Duplicate samples of each DNA were also digested with Eco RI (without Dpn I) to allow determination of the relative amount of total plasmid DNA that had replicated. These samples were separated by electrophoresis, blotted, and hybridized with pBKS$^-$ DNA probe. Replication of recombinant plasmids was demonstrated if the probe hybridized to Dpn I–resistant bands of identical size to the Eco RI–digested input plasmid DNA (Fig. 2A). Both pAcHdQ and pAcHdQL, which con-

M. Pearson, R. Bjornson, G. Rohrmann, Department of Agricultural Chemistry, Oregon State University, Corvallis, OR 97331.
G. Pearson, Department of Biochemistry and Biophysics, Oregon State University, Corvallis, OR 97331.

*To whom correspondence should be addressed.

tain the complete *hr*5 with all six palindromes, showed relatively high levels of replication, whereas pAcHdQR, which contains the right end of pAcHdQ and which lacks *hr* sequences, showed no evidence of replication. Plasmids pBG8 (with four palindromes) and pGR59 (with two palindromes) showed substantial but reduced replication. Plasmid pGR63, which contains one complete palindrome, showed low relative levels of replication. In contrast, pGR60, which is lacking 6 bp from the right end of the *hr*5-F palindrome, and plasmids pBS$^-$ (pBluescribe, Stratagene) and pBKS$^-$ showed no evidence of replication. Additional controls (Fig. 2B) indicated the following: There is no hybridization of the probe to infected or uninfected cellular DNA; pAcHdQ does not replicate when transfected into uninfected cells; and under the conditions used here, Dpn I digestion was complete. Other assays were performed on the samples with Dpn I and a restriction enzyme with a single site outside of the insert DNA. These experiments always yielded a signal of the size expected for nonintegrated plasmid DNA and ruled out simple homologous recombination as an explanation for the Dpn I–resistant signal.

To determine if other *hrs* present in the AcMNPV genome are also capable of promoting plasmid replication, we transfected a plasmid containing the 3.5-kb Pst I-J fragment into AcMNPV-infected Sf9 cells.

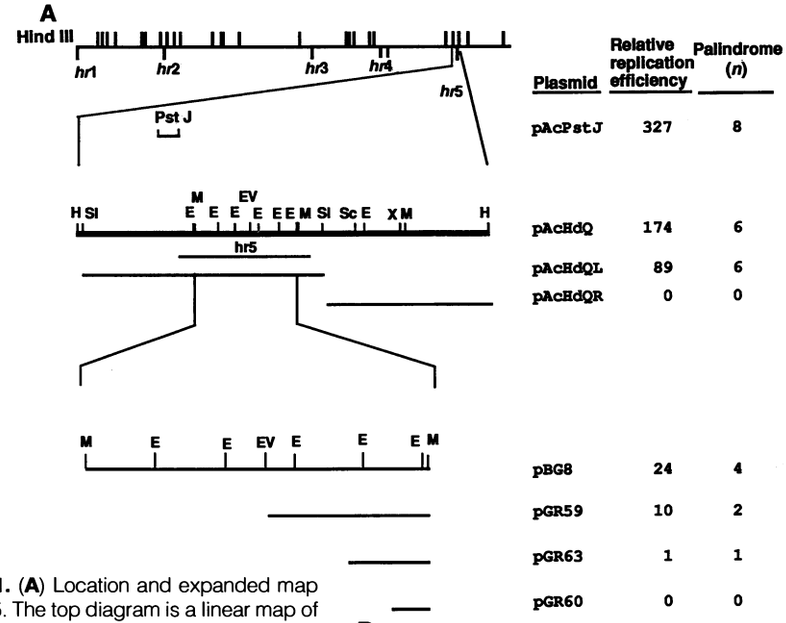

Fig. 1. (**A**) Location and expanded map of *hr*5. The top diagram is a linear map of the entire 128-kb AcMNPV genome showing the location of *hr* sequences and Hind III sites (vertical bars). Expanded from this is a map of the 2.2-kb Hind III-Q region. The locations of the 600-bp *hr*5 and subclones are indicated. Abbreviations: E, Eco RI; EV, Eco RV; H, Hind III; M, Mlu I; Sc, Sac I; SI, Sal I; and X, Xho I. We determined the replication efficiency by quantifying the Dpn I–resistant signal from a set of replication assays with a Radioanalytic Imager (AMBIS, San Diego, California). We determined the values presented by dividing the values determined for each plasmid by that of pGR63 after subtracting background counts. (**B**) The nucleotide sequence of the *hr*5 region (*7, 8*). The six palindromes (*hr*5-A through *hr*5-F) are boxed, and the dots above nucleotides indicate mismatches within the palindrome. The end points of the subclones used here are indicated by arrows. Plasmid pAcHdQ contains the AcMNPV Hind III-Q fragment cloned into pBKS$^-$. Sal I subclones of Hind III-Q (pAcHdQL and pAcHdQR) were derived from pAcHdQ. Plasmid BG8 (*9*) contains the 473-bp Mlu I fragment of AcHdQ cloned in pBS$^-$. We derived subclones pGR59, pGR63, and pGR60 by cleavage of pBG8 with Kpn I and Eco RV and then by exonuclease III digestion (*10*).

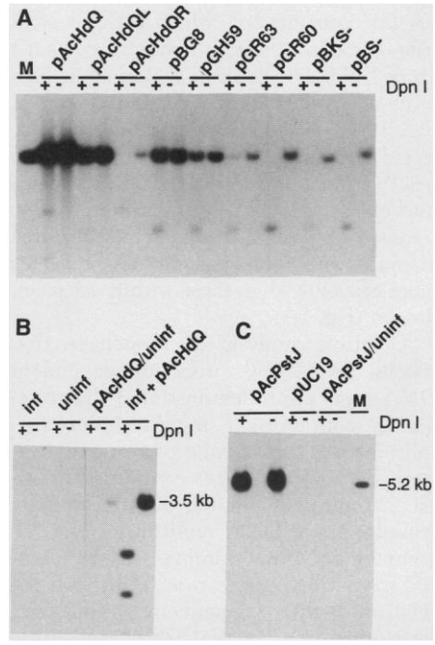

Fig. 2. Identification and characterization of an AcMNPV replication origin. (**A**) Characterization of subclones of AcMNPV Hind III-Q transfected into AcMNPV-infected Sf9 cells. Lane M is marker DNA (Eco RI–cut pAcHdQ). Each subsequent designation represents two lanes containing duplicate samples of Eco RI–cut DNA that were treated ± Dpn I. (**B**) Additional controls. Lanes: infected (inf) and uninfected (uninf) cell DNA from nontransfected cells; uninfected cells transfected with pAcHdQ (pAcHdQ/uninf); Dpn I digestion control (inf + pAcHdQ). (**C**) Characterization of the replication of AcMNPV PstJ. Lanes: pAcPstJ (cloned in pUC9) and pUC19 transfected into infected cells, and pAcPstJ transfected into uninfected cells (pAcPstJ/uninf). Lane M is marker DNA (Eco RI–cut pAcPstJ). The approximate size of the Eco RI–digested plasmid DNA is 5.2 kb. Sf9 cells (1.2 × 10^6 cells per well in six-well culture plates) incubated at 27°C in TNM-FH plus 10% fetal bovine serum media (*11*) were infected at a multiplicity of 10 with AcMNPV (E-2 strain). Four hours after infection, cells were transfected with plasmid DNA with calcium phosphate (*11, 12*). One microgram of pAcHdQ was used for transfection, and the amounts of other plasmid DNAs were adjusted to reflect equimolar amounts relative to pAcHdQ. After 4 hours, the transfection mixture was replaced with fresh media. After 65 hours, the DNA was purified by pronase digestion and phenol extraction. One-fifth (10 μl) of each DNA sample was digested with Dpn I and then with Eco RI. To ensure that Dpn I digestion was complete under these conditions, we mixed 10 μl of infected cell DNA with 0.2 μg of pAcHdQ, and it was digested as the other samples [(B), inf + pAcHdQ]. One-tenth of the digested DNA was separated by electrophoresis on agarose gels, blotted, hybridized for 16 to 18 hours, and washed under stringent conditions (*13*). For hybridization, pBKS$^-$ DNA labeled (*14*) with [^{32}P]dCTP (deoxycytidine triphosphate) was used. The exposure times were about 4 hours or 16 hours (A and B) at room temperature.

pAcPstJ contains *hr*2, which includes eight palindrome sequences distributed over about 1 kb of DNA (*3*). pAcPstJ replicated at high levels relative to the other plasmids (Fig. 2C). PUC19 DNA did not replicate when transfected into AcMNPV-infected Sf9 cells, and pAcPstJ did not replicate when transfected into uninfected cells. Quantification of Dpn I–resistant hybridization signals indicated that plasmids with more palindromes replicated more efficiently than those with fewer palindromes (Fig. 1A).

Deletion analysis of sequences that specify AcMNPV infection–dependent DNA replication demonstrated that a sequence containing a single complete palindrome was capable of promoting replication. Because sequences containing multiple palindromes elicit a disproportionate stimulation of DNA replication, the full complement of palindromes may be essential for optimal replication. Although the relation of the *hr*-dependent plasmid replication to in vivo viral DNA replication is not presently known, the distribution of *hrs* at intervals around the genome suggests that they may act cooperatively to accelerate the replication of the genome from as many as six different sites. Although palindrome sequences are common features of replication origins in bacteria, plasmids, phage, and eukaryotic viruses (*6*), the distribution and repetitious nature of these AcMNPV candidate-origins appear to be unusual.

REFERENCES AND NOTES

1. M. A. Cochran and P. Faulkner, *J. Virol.* **45**, 961 (1983).
2. L. A. Guarino and M. D. Summers, *ibid.* **60**, 215 (1986).
3. L. A. Guarino, M. A. Gonzalez, M. D. Summers, *ibid.*, p. 224.
4. G. E. Geier and P. Modrich, *J. Biol. Chem.* **254**, 1408 (1979).
5. K. W. C. Peden, J. M. Pipas, S. Pearson-White, D. Nathans, *Science* **209**, 1392 (1980).
6. A. Kornberg and T. A. Baker, *DNA Replication* (Freeman, New York, 1992).
7. P. D. Friesen and L. K. Miller, *J. Virol.* **61**, 2264 (1987).
8. A. Liu, J. Qin, C. Rankin, R. R. Weaver, *J. Gen. Virol.* **67**, 2565 (1986).
9. B. Glocker, R. R. Hoopes, G. F. Rohrmann, *J. Virol.* **66**, 3476 (1992).
10. S. Henikoff, *Methods Enzymol.* **155**, 156 (1987).
11. M. D. Summers and G. E. Smith, *A Manual of Methods for Baculovirus Vectors and Insect Cell Culture Procedures* (Bulletin No. 1555, Texas Agricultural Experiment Station, 1987).
12. F. L. Graham and A. J. Van Der Eb, *Virology* **52**, 456 (1973).
13. J. Sambrook, E. F. Fritsch, T. Maniatis, *Molecular Cloning: A Laboratory Manual* (Cold Spring Harbor Laboratory, Cold Spring Harbor, NY, 1989).
14. A. P. Feinberg and B. Vogelstein, *Anal. Biochem* **132**, 6 (1984).

15. Supported by grant AI21973 from NIH. This is report 9857 from the Oregon State University Agricultural Experiment Station. We thank J. Hays, D. Mosbaugh, and W. Ream for suggestions and comments on this manuscript.

9 April 1992; accepted 9 July 1992

Genesis of Acetate and Methane by Gut Bacteria of Nutritionally Diverse Termites

Alain Brauman, Matthew D. Kane, Marc Labat, John A. Breznak*

The evolution of different feeding guilds in termites is paralleled by differences in the activity of their gut microbiota. In wood-feeding termites, carbon dioxide–reducing acetogenic bacteria were found to generally outprocess carbon dioxide–reducing methanogenic bacteria for reductant (presumably hydrogen) generated during microbial fermentation in the hindgut. By contrast, acetogenesis from hydrogen and carbon dioxide was of little significance in fungus-growing and soil-feeding termites, which evolved more methane than their wood- and grass-feeding counterparts. Given the large biomass of termites on the earth and especially in the tropics, these findings should help refine global estimates of carbon dioxide reduction in anoxic habitats and the contribution of termite emissions to atmospheric methane concentrations.

Although generally recognized for their ability to thrive on a diet of wood, the feeding behavior and nutritional ecology of termites is quite diverse and not limited to xylophagy. Some species forage for grass and leaves, whereas others feed exclusively on soil, presumably deriving nutrition from the humic compounds therein (*1*, *2*). Still others cultivate and consume cellulolytic fungi, which, when ingested with plant materials, augment the digestive enzymes of the insect (*3*). Nevertheless, all known termites have a dense and diverse hindgut microbial community, which aids in digestion and which is the source of fermentation products such as acetate, methane (CH_4), and H_2 (*4*).

The symbiotic hindgut microflora of wood-eating, "lower" termites (for example, *Reticulitermes flavipes*) includes protozoa and bacteria and effects an essentially homoacetic fermentation of wood polysaccharide (principally cellulose) consumed by the insect. Cellulolytic protozoa first hydrolyze cellulose and ferment each glucose monomer to acetate, carbon dioxide (CO_2), and H_2 (*5*):

$$C_6H_{12}O_6 + 2\ H_2O \rightarrow 2\ CH_3COOH + 2\ CO_2 + 4\ H_2$$

then CO_2-reducing acetogenic bacteria convert H_2 and CO_2 to an additional acetate molecule (*6*):

$$4\ H_2 + 2\ CO_2 \rightarrow CH_3COOH + 2\ H_2O$$

The three net acetates formed per glucose monomer are absorbed from the hindgut and oxidized by the termite to support up to 100% of the insect's respiratory requirement (*7*):

$$3\ CH_3COOH + 6\ O_2 \rightarrow 6\ CO_2 + 6\ H_2O$$

Both H_2 and CH_4 (the latter formed by reduction of CO_2 by methanogenic bacteria) are also emitted by termites, and the extent to which termites contribute to global increases in atmospheric CH_4 has been hotly debated (*8*–*14*). However, emission of these gases represents only a small part of reduction equivalents ($H^+ + e^-$) generated by microbial fermentation in the hindgut of *R. flavipes* (*7*). In limited studies of other wood-eating "lower" and "higher" termites (the latter of which contain only bacteria in their hindguts), a similar pattern was observed (*6*). This in itself was surprising, because, in most anoxic habitats low in sulfate and nitrate, CO_2 reduction to CH_4 (not acetate) is the dominant H_2-consuming process (*15*). Therefore, to determine whether bacterial acetogenesis, rather than methanogenesis, was the major H_2-consuming "electron sink" reaction of hindgut fermentation of termites in general, we examined a variety of tropical species representing different feeding guilds (different patterns of food resource preference). Because opportunities to collect fresh specimens of many of the species (especially those from remote regions) were rare, our sampling strategy in the time available was to maximize species diversity within a particular feeding guild rather than to sample repeatedly a given species from different sites for replicate analyses. Included in this study were wood-feeding members of three families of "lower" termites (Hodo-, Kalo- and Rhinotermitidae), and wood-, grass-, and soil-feeding and fungus-growing representatives of the higher termite family Termitidae, which includes about three-quarters of all known termite species (*1*, *2*).

We quantified acetogenesis from CO_2 by measuring the reduction of $^{14}CO_2$ to ^{14}C-acetate by anoxic suspensions of termite gut contents. This was done under two conditions: (i) in the presence of exogenously

A. Brauman and M. Labat, Laboratoire de Microbiologie, Office de la Recherche Scientifique et Technique d'Outre-Mer (ORSTOM), Université de Provence, 1331 Marseille Cedex 3, France, and Laboratoire de Microbiologie, ORSTOM, Brazzaville, Republic of Congo. M. D. Kane and J. A. Breznak, Department of Microbiology and Center for Microbial Ecology, Michigan State University, East Lansing, MI 48824.

*To whom correspondence should be addressed.